

Nonadiabatic quantum wave packet dynamics of the H + H₂ reaction including the coriolis coupling[†]

B JAYACHANDER RAO and S MAHAPATRA*

School of Chemistry, University of Hyderabad, Hyderabad 500 046

e-mail: smsc@uohyd.ernet.in

Abstract. The effect of coriolis coupling on the dynamics of H + H₂ reaction is examined by calculating the initial state-selected and energy resolved reaction probabilities on the coupled manifold of its degenerate $2p$ (E') ground electronic state. H₃ in this state is prone to the Jahn–Teller (JT) instability and consequently the degeneracy is split upon distortion from its D_{3h} equilibrium geometry. The orbital degeneracy is, however, restored along the D_{3h} symmetry configuration and it results into conical intersections of the two JT split component states. The energetically lower adiabatic component of latter is repulsive, and mainly (‘rather solely’) drive the H + H₂ reaction dynamics. On the otherhand, the upper adiabatic component is of bound type and can only impart non-adiabaticity on the dynamics of lower state. Comparison calculations are therefore also carried out on the uncoupled lower adiabatic sheet to assess the nonadiabatic effect. Exact quantum scattering calculations are performed by a chebyshev polynomial propagator and employing the double many body expansion potential energy surface of the electronic ground state of H₃. Reaction probabilities are reported up to a total energy of ~ 3.0 eV, slightly above the energetic minimum of the seam of conical intersections at ~ 2.74 eV. Reaction probabilities are calculated up to the total angular momentum, $J = 20$ and for each value of J , the projection quantum number K is varied from 0 to $\min(J, K_{\max})$, with $K_{\max} = 4$. Probability results are compared and discussed with those obtained without the coriolis coupling.

Keywords. Conical intersections; nonadiabatic reaction dynamics; coriolis coupling.

1. Introduction

The H + H₂ → H₂ + H exchange reaction has been and still is the cornerstone in the experimental and theoretical research in the gas phase chemical reaction dynamics.¹ Despite some satisfactory agreements between the theory and experiment,¹ there remains several unresolved issues which invited renewed attention on this system in recent years. The most important concern at present is to unravel the electronic nonadiabatic effects on its reaction dynamics. This reaction occurs on an orbitally degenerate, $2p$ (E'), electronic state which is prone to the Jahn–Teller (JT) instability.² The resulting JT split component states form conical intersections (CIs)^{3–5} at the undistorted D_{3h} equilibrium configuration of H₃. The presence of CIs induces a geometric phase (GP) (a particular case of Berry’s phase),⁶ change (a sign change) of the adiabatic electronic wavefunction when encircling a close loop around the CIs in the nuclear configuration space.³ This issue has been re-

peatedly addressed in the recent quantum dynamical studies of the H + H₂ reaction.^{7–11} The outcome of these studies confirmed no significant GP effects in the integral reaction cross sections and in the full differential cross sections below a collision energy of 1.8 eV.^{8–11} The GP effects observed in the state-to-state reaction probabilities cancel out when the contributions from different partial waves of the total angular momentum J are summed up to obtain the reaction cross-sections.^{8–11}

The GP change accounts a part of the electronic nonadiabatic coupling and more complete studies including the two coupled surfaces explicitly was initiated by us in the past years.^{12–15} The integral reaction cross sections are reported from the onset of the reaction to the three-body dissociation limit reveal no significant nonadiabatic effects due to CIs on the reaction dynamics.^{13,15} These results are found to be in accordance with the GP results discussed above. The above mentioned studies are carried out within the centrifugal sudden or coupled states (CS) approximation.¹⁶ The mystery of insignificant effect of the nonadiabatic coupling on the H + H₂ reaction dynamics is not completely under-

[†]Dedicated to the memory of the late Professor S K Rangarajan

*For correspondence

stood yet. Therefore we attempt here to carry out an exact quantum dynamical study including the coriolis coupling (CC) to venture into this mystery. The work presented below, extends our earlier one¹³ on the same subject by including the CC in the Hamiltonian.

The role of CC in the quantum dynamics has been investigated in the past literature.^{17–23} Sukiasyan *et al*²⁴ have calculated the reaction cross sections for the H + D₂ ($\nu = 1$) and D + H₂ ($\nu = 1$) reactions on the London–Sato–Truhlar–Horowitz surface²⁵ by the multi-configuration time-dependent Hartree wave packet propagation method. These authors have found that the CC modifies the variation of reaction cross sections with reagent rotational excitation as compared to the CS results. Chu *et al*²⁶ have calculated the state-to-state integral and differential cross sections of the H + D₂ reaction on the BKMP2²⁷ surface and demonstrated that both the energy and angular dependence of the calculated cross sections are sensitive to the CC. The above studies^{24,26} were performed on the uncoupled lower repulsive adiabatic sheet of the electronic ground state of the H₃. Recently, Althorpe and coworkers²⁸ have reported the state-to-state reaction probabilities, differential cross sections and integral reaction cross sections of the H + H₂ reaction for the total energies up to 4.5 eV above the ground state minimum including the surface coupling. Their findings also reveal a similar (as in ref. 13), viz. minor impact of the nonadiabatic coupling on the integral and differential reaction sections.

It is therefore well-established that the nonadiabatic coupling effects on the H + H₂ reaction cross sections are minor. In order to get further insight on this, we set out to examine the initial state-selected and energy resolved reaction probabilities, integral reaction cross sections and thermal rate constants by carrying out exact quantum mechanical treatment of the dynamics including the CC. In the following, we only show and discuss the reaction probability data and compare them with the CS results published earlier.¹³ More calculations are necessary and are currently underway in our group to arrive at the converged reaction cross sections and the thermal rate constants in order to arrive at a final conclusion.

2. Theoretical details

The theoretical methods used here are described in our recent works^{12,13,15,23} and we do not detail them

here. Only a brief discussion on the inclusion of the CC terms in the nonadiabatic Hamiltonian and necessary modifications of the computational algorithm are provided below. As before,^{12,13,15,23} the reactant (H + H₂) Jacobi coordinates (R, r, γ) are employed in the scattering studies defining R , the distance of the H atom from the center of mass of the H₂ reagent, r the internuclear distance of H₂ and γ the angle between \vec{R} and \vec{r} . A mixed grid/basis set representation is used to numerically solve the time-dependent Schrödinger equation (TDSE)

$$|\psi(t)\rangle = \exp[-i\hat{H}t/\hbar]|\psi(t=0)\rangle, \quad (1)$$

where $|\psi(t)\rangle$ is the wavefunction of the reacting system at time t and \hat{H} is the Hamiltonian operator of the collisional system which is explicitly time-independent. This Hamiltonian for the coupled electronic ground state of H₃ is written in a diabatic electronic basis as

$$\hat{H}^d = \hat{T}_N \begin{pmatrix} 1 & 0 \\ 0 & 1 \end{pmatrix} + \begin{pmatrix} U_{11} & U_{12} \\ U_{21} & U_{22} \end{pmatrix} \quad (2)$$

where \hat{T}_N represents the nuclear kinetic energy operator (which is diagonal in the diabatic basis) and is given by

$$\hat{T}_N = -\hbar^2/2\mu[\partial^2/\partial R^2 + \partial^2/\partial r^2] + \hat{j}^2/2\mu r^2 + \hat{l}^2/2\mu R^2. \quad (3)$$

The quantities U_{11} and U_{12} in (2) are the energies of the two diabatic electronic states and, $U_{12} = U_{21}$ represent their coupling potential. In (3), the operator \hat{j} defines the diatomic rotational angular momentum associated with the Jacobi angle γ , and \hat{l} is the orbital angular momentum operator. The quantity, $\mu = m_H/\sqrt{3}$ (m_H is the mass of the H atom), is a scaled three-body reduced mass. The BF z -axis is defined to be parallel to \hat{R} and the diatom lies in the (x, z) plane. The quantity \hat{l}^2 is given as

$$\hat{l}^2 \equiv (\hat{J} - \hat{j})^2 = \hat{J}^2 + \hat{j}^2 - 2\hat{J}_z\hat{j}_z - \hat{J}_+\hat{j}_- - \hat{J}_-\hat{j}_+, \quad (4)$$

where \hat{J} is the total angular momentum operator and \hat{J}_z and \hat{j}_z are the respective BF z -components of \hat{J} and \hat{j} . \hat{J}_+ (\hat{J}_-) and \hat{j}_+ (\hat{j}_-) are the corresponding raising (lowering) operators. The last two terms in (4) are known as coriolis coupling terms. Within the CS approximation, these two terms in the Hamilto-

nian are neglected. In this approximation K (the projection of \hat{J} and also \hat{j} on the BF z -axis) remains a good quantum number and treated as a parameter. In the present investigations, we include these CC terms allowing a coupling between neighbouring K states in the quantum dynamics of the H + H₂ reaction and compare the results with those obtained in ref. 13 (within the CS approximation).

The initial wave packet (WP), $|\psi(t=0)\rangle$ corresponding to the reagent H + H₂ is prepared in the asymptotic reagent channel (at large R) of the repulsive lower adiabatic sheet, V_- , of the DMBE PES. Asymptotically, $|\psi(t=0)\rangle$ is expressed as a product of the translational Gaussian WP (for the motion along R) and the rovibrational wave function of H₂ molecule in a similar way as discussed in Ref. 13. This adiabatic wavefunction is transformed to the diabatic electronic basis, $|\psi\rangle^d = \mathbf{S} |\psi\rangle^{ad}$; with

$$\mathbf{S} = \begin{pmatrix} \cos\theta & \sin\theta \\ -\sin\theta & \cos\theta \end{pmatrix},$$

and propagated in the coupled manifold of electronic states of (2). The diabatic electronic matrix of the latter is obtained from the adiabatic potentials (V_{\pm}) of the DMBE PES with the aid of the following unitary transformation

$$\begin{pmatrix} U_{11} & U_{12} \\ U_{21} & U_{22} \end{pmatrix} = \mathbf{S} \begin{pmatrix} V_- & 0 \\ 0 & V_+ \end{pmatrix} \mathbf{S}^\dagger \quad (5)$$

$$= \frac{V_- + V_+}{2} \mathbf{1} + \frac{V_+ - V_-}{2} \begin{pmatrix} -\cos\chi & \sin\chi \\ \sin\chi & \cos\chi \end{pmatrix}, \quad (6)$$

where χ represents the pseudorotation angle and within a linear coupling scheme it is twice the adiabatic-to-diabatic mixing angle θ .^{29–31}

The reaction probabilities are calculated from the flux of the scattered WP at the asymptotic product channel (at large $r = r_d$). In a diabatic electronic basis the total probability of the reaction starting from a given initial state (i) of the reagent is given by^{12,32}

$$P_i^R(E) = \frac{\hbar}{\mu} \sum_{k=1}^2 \text{Im}[\langle \phi_k^d(R, r_d, \gamma, E) | \partial \phi_k^d(R, r_d, \gamma, E) / \partial r \rangle] |_{r=r_d}, \quad (7)$$

where $\phi_k^d(R, r_d, \gamma, E)$ is the energy normalized wavefunction obtained by the Fourier transform of the

time-evolved WP at $r = r_d$. The quantity in the right hand side of (7) is integrated over the entire range of R and γ and the summation runs over the two participating diabatic electronic states.

Numerical solution of the TDSE is carried out by constructing a grid in the (R, r, γ) space. The grid consists of 128 and 64 equidistant points along R and r , respectively, with $0.1a_0 \leq R \leq 15.34a_0$ and $0.5a_0 \leq r \leq 8.06a_0$. The fast Fourier transform method³³ is used to evaluate the action of the kinetic energy operator on the wavefunction along these radial coordinates. The action of the kinetic energy operator along γ is carried out by the Gauss–Legendre discrete variable representation method³⁴ with 48 quadrature points. The time propagation of the WP is carried out by the chebyshev polynomial method.³⁵ The initial WP is located at $R = 10.5a_0$ and the width parameter of the GWP is set to $0.16a_0$. The flux of the scattered WP is collected at $r_d = 4.10a_0$. The WP is propagated for a total of 4.14 ps with a time step of 0.135 fs. At each time the fast moving components of the WP reaching the grid boundaries are absorbed by activating a sine type of damping function at $R = 11.62a_0$ and $r = 4.7a_0$. The efficiency of such a damping function is already discussed in detail in a previous publication.³⁶

3. Results and discussion

The WP calculations including the CC for bimolecular reactive scattering process is well-known to be computationally very intensive. In addition, the present investigations consider nonadiabatic coupling of two electronic states. Therefore, the computational overhead raises by a factor of two for each WP propagation, compared to the single surface calculations. For example, the WP propagation on a single adiabatic PES for ~ 4.14 ps for a given J requires ~ 60 h of CPU time (on a single processor) in a IBM P690 machine. This CPU hours nearly doubles when the dynamics is simulated on the two coupled PESs. A parallelization of the algorithm to reduce the computational time is left for a future work. In the following, we show and discuss some reaction probability results. More calculations of probabilities for further higher K values are necessary to obtain the converged integral reaction cross sections and thermal rate constants. Such calculations are presently ongoing in our group. The calculations reported below are carried out with $K_{\text{max}} = 4$ and the reagent H₂ in its vibrational and rotational ground state. The

probabilities are calculated up to a total energy of 3.0 eV. Partial wave contributions for the total angular momentum up to $J=20$ are estimated to be required to obtain the converged reaction cross sections up to this energy. This is illustrated in figure 1 by plotting the J dependence of the degeneracy $(2J+1)$ weighted probability for the $\text{H} + \text{H}_2$ ($\nu=0, j=0$) reaction for five different values of the total energy indicated in the panel.

The initial state-selected and energy resolved reaction probability for $\text{H} + \text{H}_2$ ($\nu=0, j=0$) as a function of the total energy E obtained on the uncoupled lower adiabatic surface are plotted in figure 2a–b for the total angular momentum, $J=1$ and $K=0$, in panel (a) and $K=1$, in panel (b), respectively. In each panel, the results obtained within the CS approximation and by including the CC are shown by the solid and dashed lines, respectively. In the CS calculations, K is fixed whereas, in the CC calculations K is a variable quantity and is allowed to vary between 0 to $\min(J, K_{\max})$. We can see from figure 2a–b that both CC and CS reaction probabilities show similar resonance pattern. The location of these resonances differ in both the cases which can be seen from figure 2a–b. A shift of the location of the resonances to higher energies in presence of CC is demonstrated in a recent study by Padmanaban and Mahapatra.³⁷ Also, the resonances tend to become broader when CC is included in the dynamics.³⁷ The results presented in figure 2a–b are in accordance with these observations.

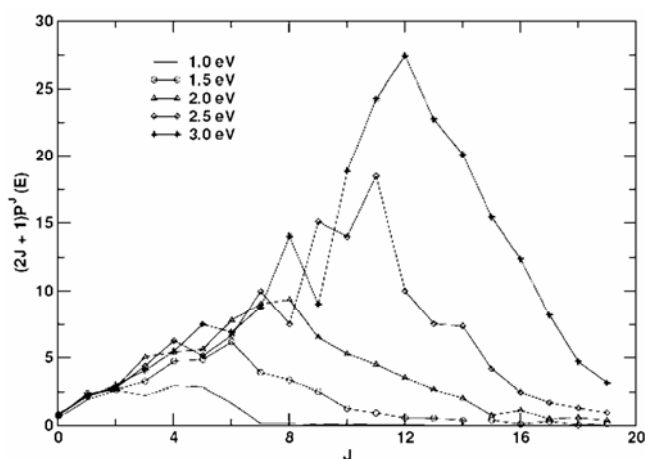


Figure 1. Weighed partial wave contribution to the integral reaction cross sections at various values of the total energies (indicated in the panel) for the $\text{H} + \text{H}_2$ ($\nu=0, j=0$) reaction.

The above reaction probabilities obtained in the coupled surface situations are shown in figure 3a–b. Again the results obtained within the CS approximation and including the CC are shown by the solid and dashed lines, respectively. For comparison the uncoupled surface results including the CC (shown in figure 2) are also included in each panel and shown by the dotted lines. The difference between the CC and CS results seems to reduce for higher K values. Again as it was generally found before,^{12–15,28} that the coupled and uncoupled surface results do not show large difference implying a mild effect of the surface coupling on the $\text{H} + \text{H}_2$ reaction dynamics. A similar observation of insignificant effect of GP on the coriolis coupling terms of the Hamiltonian for the $\text{H} + \text{H}_2$ reaction is also assessed by Althorpe and coworkers.²⁸

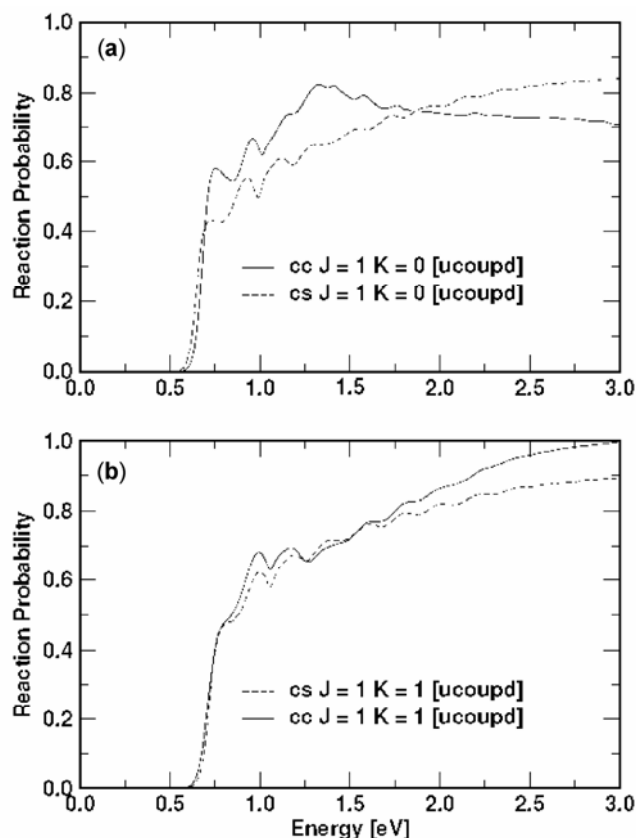


Figure 2. The $\text{H} + \text{H}_2$ ($\nu=0, j=0$) reaction probabilities calculated on the uncoupled lower adiabatic surface as a function of the total energy ($\text{H} - \text{H}_2$ translational energy + H_2 rovibrational energy) for the total angular momentum $J=1, K=0$, in panel (a) and $J=1, K=1$, in panel (b). The results obtained including the CC and within the CS approximation are shown by solid and dashed lines, respectively.

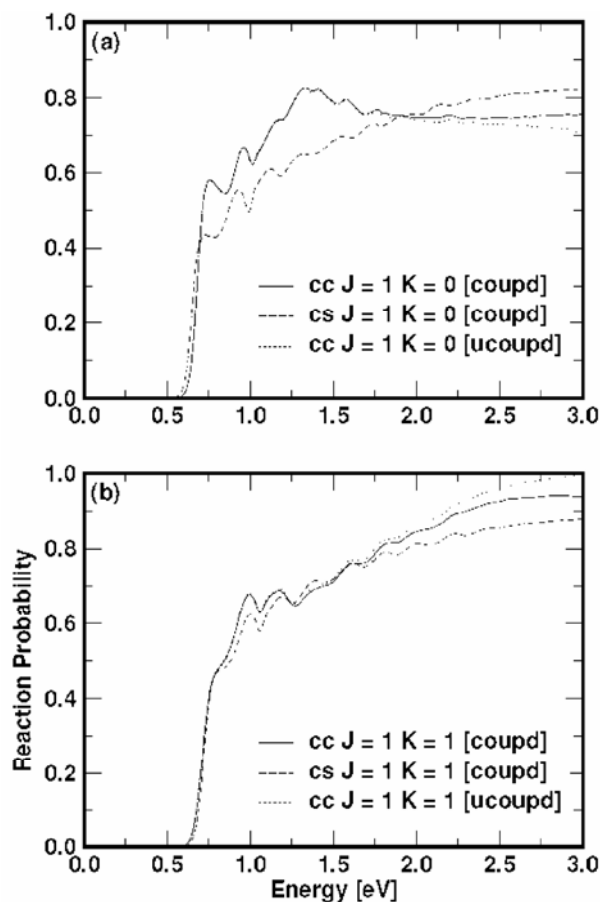


Figure 3. Same as in figure 1 calculated in the coupled surface situation. The uncoupled surface CC results of figure 1 are also included and shown as dotted lines in both the panels for a clear comparison.

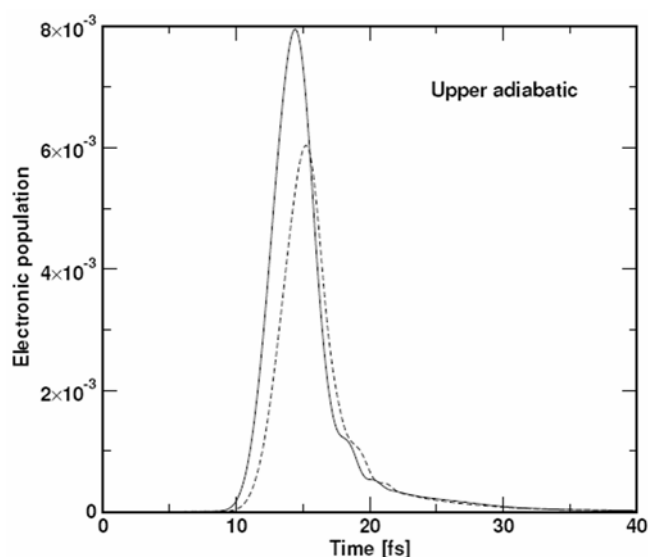


Figure 4. Time-dependence of the electronic population of the upper adiabatic sheet V_+ during the course of the $H + H_2$ ($v = 0, j = 0$) $\rightarrow H_2$ ($\Sigma v', \Sigma j'$) + H reaction for $J = 1$ and $K = 0$. The CC and CS results are shown by the solid and dashed lines, respectively.

The time-dependence of the population of the upper adiabatic sheet V_+ in the coupled surface dynamics of the $H + H_2$ ($v = 0, j = 0$) reaction for $J = 1, K = 0$ case is shown in figure 4. The CC and CS results are shown by solid and dashed lines, respectively. It can be seen from the figure that the CC causes only a slight increase of the WP density in the upper adiabatic state and the maximum of the population curve occurs slightly earlier (by ~ 0.85 fs) when compared to the CS results.

The coriolis-coupled initial state-selected $H + H_2$ ($v = 0, j = 0$) reaction probabilities calculated in both coupled and uncoupled surface situations for $J = 5$ and $K = 0$ to 4 are shown in figures 5a–e. The coupled and uncoupled surface results are shown by the full and dashed lines, respectively. It can be seen from figure 5a–e that the difference between the coupled and uncoupled reaction probabilities increases with an increase in the K value. But as J increases, the difference between the coupled and

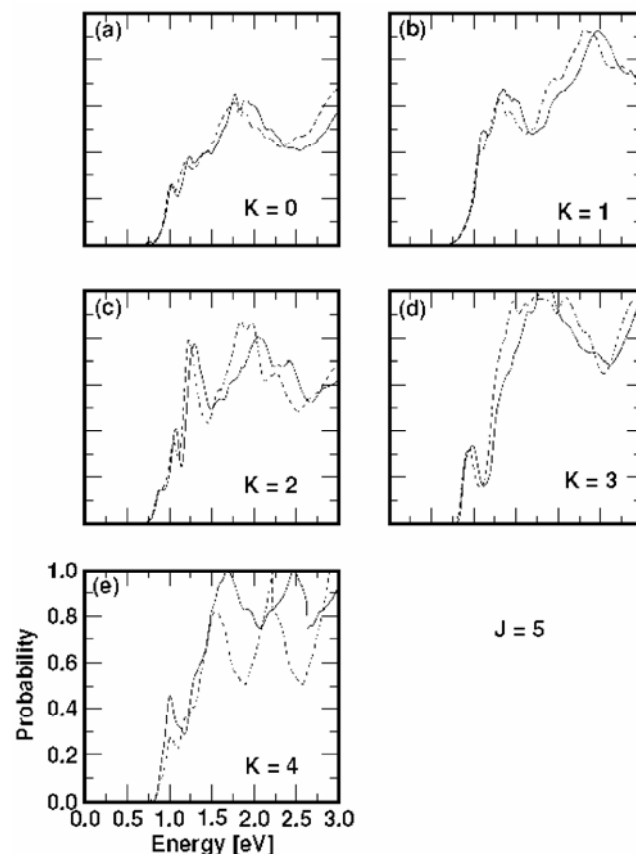


Figure 5. Coriolis-coupled reaction probabilities as a function of total energy for the $H + H_2$ ($v = 0, j = 0$) reaction for $J = 5, K = 0-4$, are shown in panels (a)–(e), respectively. The coupled and uncoupled surface results are shown by the full and dashed lines, respectively.

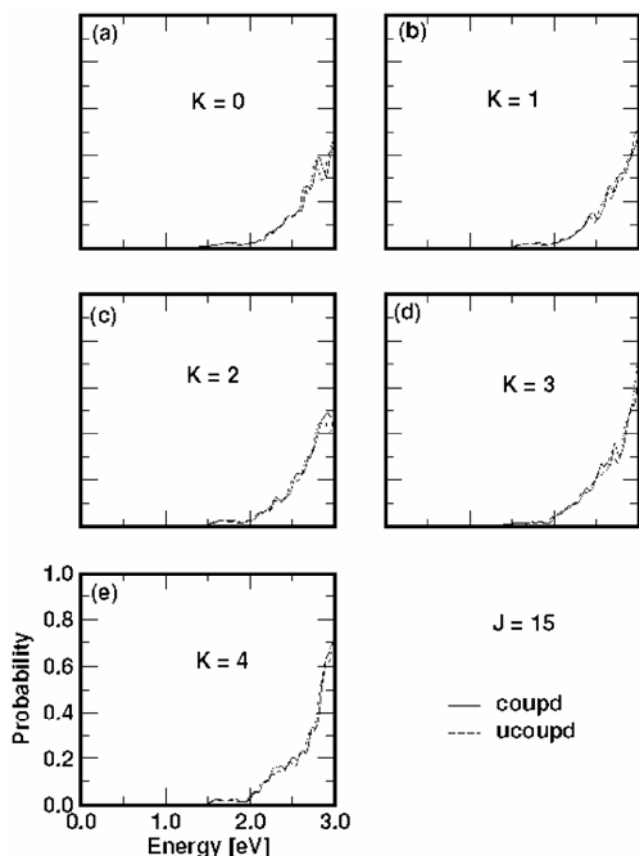


Figure 6. Same as in figure 5, for $J = 15$, $K = 0-4$.

uncoupled surface results reduces for any value of K from 0 to K_{\max} . This can be seen from figure 6a–e in which the coriolis-coupled reaction probabilities for $J = 15$ and $K = 0$ to 4 are plotted. As above, the coupled and uncoupled surface results are shown by the full and dashed lines, respectively.

In summary, we have presented a preliminary account of an exact quantum wave packet study of the $H + H_2$ reaction using the DMBE PES of H_3 both with and without including the surface coupling in the dynamics. The reaction probabilities are calculated up to the total energy of ~ 3.0 eV. The results of these calculations are compared with those which ignore the CC terms in the Hamiltonian. The latter do not reveal any significant impact on the non-adiabatic dynamics of $H + H_2$. The CC and CS reaction probabilities show similar resonance pattern. The resonances tend to become broader when the CC is included. More calculations for further higher values of K are presently being carried out in order to obtain converged integral reaction cross sections and thermal rate constants.

Acknowledgements

This study is supported in part by a research grant from the Department of Science and Technology (DST), New Delhi (Grant No. DST/SF/04/2006). The computational facilities provided by the Center for Modelling Simulation and Design (CMSD), University of Hyderabad is gratefully acknowledged. BJR thanks the Council of Scientific and Industrial Research (CSIR), New Delhi for a Senior Research Fellowship.

References

1. Fernández-Alonso F and Zare R N 2002 *Ann. Rev. Phys. Chem.* **53** 67; Aoiz F J, Bañares L and Herrero V J 2005 *Int. Rev. Phys. Chem.* **24** 119 and references therein
2. Jahn H and Teller E 1937 *Proc. Roy. Soc. London, Ser. A* **161** 220
3. Herzberg G and Longuet-Higgins H C 1963 *Discuss. Faraday. Soc.* **35** 77
4. *Chemical Physics* **259** 121–350, 2000 (special issue on conical intersections: *Conical Intersections in Photochemistry, Spectroscopy and Chemical Dynamics*)
5. Domcke W, Yarkony D R and Köppel H (eds) 2004 *Conical intersections: Electronic structure, dynamics and spectroscopy* (Singapore: World Scientific)
6. Berry M V 1984 *Proc. Roy. Soc. London, Ser. A* **392** 45
7. Kupperman A and Wu Y M 2001 *Chem. Phys. Lett.* **349** 537
8. Kendrick B K 2000 *J. Chem. Phys.* **112** 5679; Kendrick B K 2003 *J. Phys. Chem.* **A107** 6739; Kendrick B K 2003 *J. Chem. Phys.* **118** 10502
9. Juanes-Marcos J C and Althorpe S C 2005 *J. Chem. Phys.* **122** 204324
10. Juanes-Marcos J C, Althorpe S C and Wrede E 2005 *Science* **309** 1227
11. Althorpe S C, Juanes-Marcos J C and Wrede E 2008 *Adv. Chem. Phys.* **138** 1
12. Mahapatra S, Köppel H and Cederbaum L S 2001 *J. Phys. Chem.* **A105** 2321
13. Jayachander Rao B, Padmanaban R and Mahapatra S 2007 *Chem. Phys.* **333** 135
14. Ghosal S, Jayachander Rao B and Mahapatra S 2007 *J. Chem. Sci.* **119** 401
15. Jayachander Rao B and Mahapatra S 2007 *Indian. J. Phys.* **81** 1003
16. Pack R T 1974 *J. Chem. Phys.* **60** 633; McGuire P and Kouri D J 1974 *J. Chem. Phys.* **60** 2488
17. Meijer A J H M and Goldfield E M 1999 *J. Chem. Phys.* **110** 870
18. Carroll T E and Goldfield E M 2001 *J. Phys. Chem.* **A105** 2251
19. Morari H and Jaquet R 2005 *J. Phys. Chem.* **A109** 3396
20. Zhang H and Smith S C 2004 *Phys. Chem. Chem. Phys.* **6** 4240

21. Xie T X, Zhang Y and Han K L 2004 *Chin. J. Chem. Phys.* **17** 657
22. Zhang Y, Xie T X, Han K L and Zhang J Z H 2003 *J. Chem. Phys.* **119** 12921; Chu T S, Zhang Y and Han K L 2006 *Int. Rev. Phys. Chem.* **25** 201; Chu T S and Han K L 2008 *Phys. Chem. Chem. Phys.* **10** 2431
23. Padmanaban R and Mahapatra S 2006 *J. Phys. Chem.* **A110** 6039
24. Sukiasyan S and Meyer H-D 2002 *J. Chem. Phys.* **116** 10641
25. Truhlar D G and Horowitz C 1978 *J. Chem. Phys.* **68** 2466; Truhlar D G and Horowitz C 1979 *J. Chem. Phys.* **71** 1514
26. Chu T S, Han K L, Hankel M and Gabriel G Balint-Kurti 2007 *J. Chem. Phys.* **126** 214303
27. Boothroyd A L, Keogh W J, Martin P G and Peterson M R 1991 *J. Chem. Phys.* **104** 7139
28. Bouakline F, Althorpe S C and Peláez Ruiz D 2008 *J. Chem. Phys.* **128** 124322
29. Thiel A and Köppel H 1999 *J. Chem. Phys.* **110** 9371
30. Köppel H, Gronki J and Mahapatra S 2001 *J. Chem. Phys.* **115** 23771
31. Mahapatra S and Köppel H 1998 *J. Chem. Phys.* **109** 1721
32. Mahapatra S 2004 Quantum reaction dynamics on multi-sheeted potential energy surfaces. In *Conical intersections: Electronic structure, dynamics and spectroscopy* (eds) W Domcke, D R Yarkony and H Köppel (Singapore: World Scientific) pp 555–581
33. Kosloff D and Kosloff R 1983 *J. Comput. Chem.* **52** 35
34. Light J C, Hamilton I P and Lill J V 1985 *J. Chem. Phys.* **82** 1400; Bačić Z and Light J C 1989 *Ann. Rev. Phys. Chem.* **40** 469
35. Tal-Ezer H and Kosloff R 1984 *J. Chem. Phys.* **81** 3967
36. Mahapatra S and Sathyamurthy N 1997 *J. Chem. Soc. Faraday Trans.* **93** 773
37. Padmanaban R and Mahapatra S 2006 *J. Theor. and Comput. Chem.* **5** 871